Available online at www.sciencedirect.com

ScienceDirect

Procedia Structural Integrity 25 (2020) 454–464

Structural Integrity Procedia

www.elsevier.com/locate/procedia

1st Virtual Conference on Structural Integrity – VCSI1

Strategies to improve the structural integrity of tied-arch bridges affected by instability phenomena

Domenico Ammendolea[a], Fabrizio Greco[a], Paolo Nevone Blasi[a], Paolo Lonetti[a], Arturo Pascuzzo*[a]

[a]*Department of Civil Engineering, University of Calabria, Via P. Bucci, Cubo39B, 87030, Rende, Cosenza, Italy*

Abstract

A numerical study is proposed to investigate the nonlinear behavior of steel tied-arch bridges, whose arch ribs are inclined inwardly. The main aim of the paper is to assess if the arch rib inclination may be an effective strategy to enhance the structural integrity of the bridge structure against out-of-plane buckling mechanisms. The nonlinear behavior of the structure is investigated throughout an advanced 3D finite element model, which accurately reproduces nonlinear sources involved in the cable system and structural elements. An analysis that combines results obtained by traditional elastic buckling analysis and incremental nonlinear elastic analysis is employed to properly evaluate the maximum capacity of the structure. Comparisons between bridge structures with inclined and vertical ribs configurations are proposed focusing attention on both structural and economic aspects. Results show that rib inclination provides several structural benefits to the bridge while reducing overall construction costs.

Keywords: Tied arch bridges; Buckling; Finite Element Method; Nonlinear Analysis; Inclined arch ribs; structural integrity

* Corresponding author. Tel.: +39 0984 496946
E-mail address: arturo.pascuzzo@unical.it

2452-3216 © 2020 The Authors. Published by Elsevier B.V.
This is an open access article under the CC BY-NC-ND license (http://creativecommons.org/licenses/by-nc-nd/4.0/)
Peer-review under responsibility of the VCSI1 organizers
10.1016/j.prostr.2020.04.051

Nomenclature

L	Bridge Span Length
L^R	Arch rib length
L^R_{br}	Wind bracing system length
h	Height of the end portal
B	Bridge width
f	Arch rise
α^C	Hanger slope
α^R	Arch rib slope
DL	Dead Load
LL	Live Load
H^R	Height of the arch rib cross-section
B^R	Width of the arch rib cross-section
t^R_w	Web thickness of the arch rib cross-section
t^R_f	Flange thickness of the arch rib cross-section
H^T	Height of the tie girder cross-section
B^T	Width of the tie girder cross-section
t^T_w	Web thickness of the tie girder cross-section
t^T_f	Flange thickness of the tie girder cross-section
D^{br}	External diameter of the arch cross beam
t^{br}	Thickness of the arch cross beam
m	Number of hangers
m^{br}	Number of Arch cross-beam
p	Hangers steo
p^{br}	Step of the arch cross-beam along the arch rib
A^C	Hanger cross-section
S^C	Hanger initial stress

1. Introduction

During the last decades, tied-arch bridges have become very competitive to cable-stayed bridges in the field of medium span lengths, and probably, they will be an effective solution to overcome long spans in the next future (Greco et al. (2019)). The structure of a tied arch bridge is composed of two arch ribs, which sustain a lower deck by means of several hanger cables. In particular, the deck ties the arch ribs extremities together, thus supporting the horizontal thrust (Lonetti et al. (2016); Tan and Yao (2019)). The hanger arrangement classifies tied arch bridges basically in (*i*) moment tied and (*ii*) network configurations: the first consists of several vertical hangers equally spaced along the tie girders, whereas the latter is composed of the union of two specular planes of inclined hangers forming a net configuration (Pellegrino et al. (2010); Bruno et al. (2016)).

The arch ribs are mainly subjected to compression, whereby being easily susceptible to out-of-plane buckling phenomena that may compromise the integrity of the whole structure (Lonetti and Pascuzzo (2019, 2016); Tetougueni et al. (2019, 2020)). High axial compressions may be induced by (1) heavy live loads acting on the deck, such as high-speed trains (Greco et al. (2018)), (2) ground-related risks or (3) actions induced by hazards (Greco et al. (2013); Bruno et al. (2018); Lonetti and Maletta (2018); Tetougueni and Zampieri (2019)). For this reason, the buckling design of tied-arch bridges represents one of the major issue that designers have to address. Usually, wind bracing systems are adopted to increase the capacity of the structure against out-of-plane buckling phenomena. In this framework, the most traditional configurations are (*i*) Vierendeel, (*ii*) X-shaped, and (*iii*) K-shaped schemes (Latif and Saka (2019)). However, these systems may be considerably expensive since require much material as well as long manufacturing

processes to be realized. Currently, this aspect represents the main obstacle to the application of tied-arch bridges in the field of long-span structures. Consequently, effective strategies to enhance the integrity of tied-arch bridges against out-of-plane buckling phenomena while saving economic resources are much required. Surprisingly, the out-of-plane buckling behavior of tied arch bridges has still not been extensively investigated since few research works have focused on the problem. Ju (Ju (2003)) performed a systematic study with the aim to define analytical formulas for calculating the buckling length factors of the most common arch bridge configurations, such as upper and lower deck ones. De Backer et al. (Backer et al. (2014)) investigated out-of-plane nonlinear behavior of steel tied-arch bridges by using an advanced 3d numerical model. The main aim was to assess the reliability of the simplified approach proposed by Eurocode to define the critical axial force in arch ribs. They found that numerical evaluations are less conservative than results determined by using EC3 procedures. On the base of their investigations, they proposed a practical formula for a proper evaluation of the buckling length factor. Liu et al. (Liu et al. (2014)) defined an analytic solution to evaluate the lateral buckling load for tied arch bridges braced by means of Vierendeel wind bracing layout. More recently, a numerical investigation on tied arch bridges based on nonlinear incremental elastic analyses is proposed in (Lonetti et al. (2019)), in which is shown how traditional buckling analyses may lead to overestimations in the maximum buckling capacity of the structure. While some research has been carried out on the buckling behavior of tied arch bridges, only a few studies have attempted to investigate the buckling behavior of network arch bridges (Greco et al. (2019); Lonetti and Pascuzzo (2019)). In particular, in (Lonetti and Pascuzzo (2019)), a practical method to quickly evaluate the critical axial force of network arch bridges has been proposed. It is worth noting that, previous studies mainly focused on tied-arch bridge structures based on vertical arch ribs. However, during the last years, a number of bridge configurations with inclined arch ribs is realized in practical applications (Guo et al. (2012); Ştefan Guţiu et al. (2016); Lan et al. (2019)). In particular, the arches are frequently inclined inwardly, thereby reducing the transversal distance between the top points. This configuration provides relevant aesthetic benefits to the bridge, but it also contributes to increasing the lateral stiffness of the structure. However, there is a current paucity of studies investigating the buckling capacity of the tied-arch bridge with inclined arches (Gui et al. (2016)).
The purpose of this paper is to examine the nonlinear behavior of tied-arch bridges with ribs inclined inwardly, especially focusing on the benefits induced by arches inclination on the buckling capacity of the structure. The nonlinear behavior is examined by means of a combined analysis based on traditional Elastic Buckling Analysis (EBA) and Nonlinear Elastic Analysis (NEA).
This paper begins by describing the numerical model and analysis methods employed to investigate the nonlinear behavior of tied arch bridges. It will then go on to numerical results and discussions.

2. Numerical implementation

2.1. Structural scheme of the bridge

The structural scheme depicted in Fig.1 represents a typical tied-arch bridge, in which arch ribs are inclined inwardly with an angle (α^R). The geometry of the structure is defined in terms of the span length (L), deck width (B), and rise (f). The cable system is typically arranged according to two geometric configurations: (*i*) the moment tied scheme, which consists of several vertical hangers and (*ii*) the network configuration, which is formed by the combination of two specular planes of hangers inclined of a constant slope (α^C) with respect to the horizontal axis. Both configurations ensure intermediate supports equally spaced of (p) along the girder.
Usually, the arch ribs are braced against out-of-plane displacements by means of a wind bracing system, whose typical configurations are Vierendeel, X-shaped, and K-shaped layouts. The un-braced portions of the arch ribs identify the end portals of the structure, whose height is denoted by h. The ratio between the height of the end portal and the total length of the arch ribs, i.e. h/L^R, is frequently employed as dimensionless parameter to quantify the extension of the wind bracing system. The arch rib and the tie girder typically consist of hollow rectangular cross-sections, whereas pipes are used for wind bracing system components.
The bridge presents external boundary conditions based on in-plane hinged or simply restrains at right and left ends respectively, whereas along out-of-plane direction fixed conditions are considered.
In the common practice, the cross-sections are dimensioned by means of practical design rules (Hedgren (1994)),

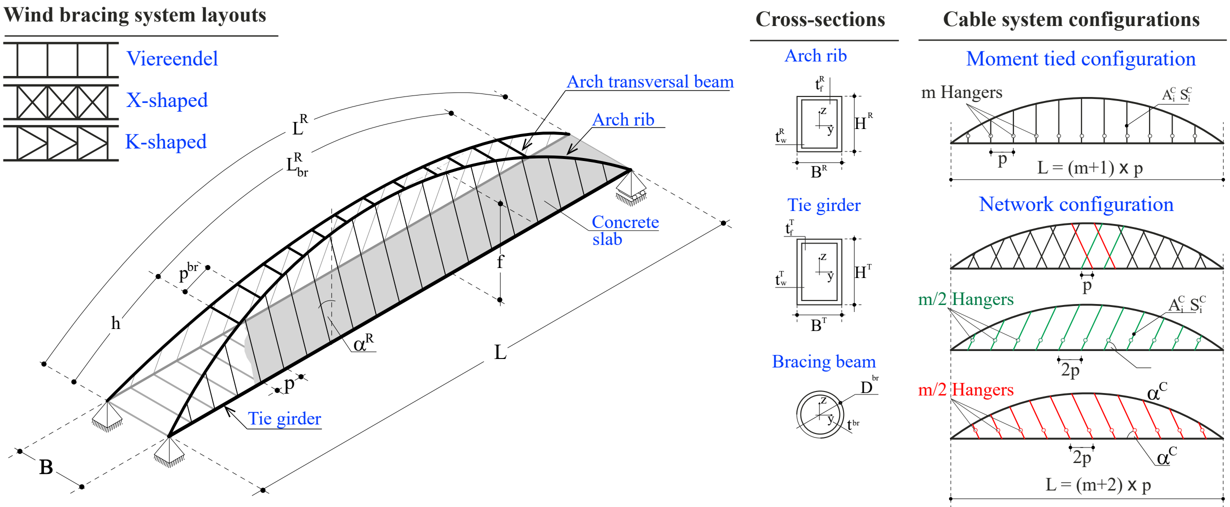

Fig. 1. A schematic of a tied-arch bridge

which were defined according to dimensions employed in most of tied-arch bridge structures build in the past (see Table 1). Similarly, preliminary design rules are defined for the wind bracing system (Table 2).

2.2. Numerical model and analysis methods

The bridge structure is analyzed by means of an advanced 3D FE model, in which the arch rib, the tie girder, and the arch transversal beams are modeled by using Timoshenko nonlinear beam elements, whereas truss elements are adopted for the hangers. In particular, the hangers are discretized into a number of elements according to the Multi Element Cable System (MECS) approach, which permits to reproduce any source of nonlinearity of cables properly. Both arch and girder are connected to the cable system by means of explicit constraint equations defined at interceptions nodes of beams and truss elements.

Usually, two methods are employed to investigate the nonlinear behavior of tied arch bridges: (*i*) an eigenvalue buckling analysis (EBA), which calculates the critical mode shapes of the structure and corresponding critical load multipliers, and (*ii*) a nonlinear elastic analysis (NEA), which consists of a step-by-step analysis where the acting loads are progressively increased up to the crisis of the structure. EBA permits to characterize the nonlinear behavior of the structure with a relatively low computational effort. However, it does not account for any nonlinear source arising from

Table 1. Preliminary design rules of the cross-sections of structural elements

Design Variables		Minimum	Maximum	Mean
Height of the arch rib cross-section to span length ratio	H^R/L	1/190	1/140	5/806
Width of the arch rib cross-section to span length ratio	B^R/L	1/190	1/140	5/806
Height of the tie girder cross-section to span length ratio	H^T/L	1/70	1/50	3/175
Cable cross-section	A^C (cm^2)	23.079	53.851	38.465

Table 2. Preliminary design rules for wind bracing system configuration

Design Variables		Minimum	Maximum	Mean
Step of the arch cross beam to bridge width ratio	p^{br}/B	1/4	3/4	1/2
Height of the end portal to arch rib length ratio	h/L^R	0.024	0.271	0.147

the cable system. On the other hand, NEA allows to properly predicting the nonlinear behavior of the structure because it reproduces any kind of nonlinear effect. However, it should be performed considering the structure subjected to initial out-of-plane displacements to accurately capture out-of-plane buckling mechanisms. Based on the previous remarks, in the present study an analysis method that combines EBA and NEA is adopted to analyze the out-of-plane nonlinear behavior of tied-arch bridges. The proposed method is described in detail in Table 3. It is worth nothing that, EBA and NEA analyses require firstly the definition of the initial configuration of the bridge structure under the action of dead loads (DL) (points 2.1 and 3.1), which consists to evaluate the initial stress distribution in hangers, arch ribs, and tie girder. This step is considerable important in the present study because the nonlinear behavior of the bridge structure is highly affected by stress and strain distribution. The identification of the initial configuration is performed by means of a numerical procedure according to "*zero displacement method*", which is usually adopted in the context of cable-supported bridges. This method identifies the initial stress distribution of hangers, arch ribs, and tie girder to reduce the deformations of the bridge structure under the action of dead loads. For sake of brevity, the numerical procedure is not discussed here, but details regarding the numerical implementation can be found in (Lonetti and Pascuzzo (2014a,b,c)).
Starting from the initial configuration, EBA calculates the live load multipliers and the corresponding critical buckling modes of the structure by solving the eigenvalue problem associated to the governing equation of the structural problem (point 2.2). In the case of NEA, once that the initial configuration of the structure is defined, initial displacements are imposed to the structure reproducing the first critical buckling mode shape (calculated by EBA in point 2.2) with a maximum magnitude of $L/8000$ (point 3.2). Note that, this magnitude is considerably smaller than $L/300$, which is the value that EC3 (European Committee for Standardization (2006)) usually prescribes to reproduce the effect of geometric imperfections. This because a magnitude of $L/300$ may highly influence the nonlinear behavior of the structure, thereby leading to relevant conservative prediction of the maximum carrying load of the structure. NEA identifies the maximum buckling load of the structure by performing an incremental analysis (point 3.3). In particular, the equilibrium equations of the structure are solved by imposing at the i-th loading step the following equations:

$$[\mathbf{K}_L + \lambda\mathbf{K}_{NL}]\,[\mathbf{u} + \Delta\mathbf{u}] = \mathbf{g}_0 + \lambda\mathbf{q} \tag{1}$$

where $\mathbf{K}_L$ is the stiffness matrix, $\mathbf{K}_{NL}$ is the stress stiffness matrix, $\mathbf{g}_0$ and $\mathbf{q}$ are the dead and live load vectors, $\mathbf{u}$ and $\Delta\mathbf{u}$ are the displacement vector and its incremental quantity, respectively.

3. Results

Numerical results are proposed with the aim to analyze the out-of-plane nonlinear behavior of tied-arch bridges, investigating the influence of arch ribs inclination on the out-of-plane buckling capacity of the structure. The study was developed with reference to a steel tied-arch bridge of 150 m, whose width (B) and rise (f) are equal to 15 m and 27 m (*i.e.* f/L=0.18), respectively. Arch ribs and tie girders are made of steel and have rectangular hollow cross-sections, whereas pipe elements are used for the beams of the wind bracing system. Table 4 summarizes cross-section dimensions, which were selected according to the mean values of preliminary design rules typically adopted in the framework of tied-arch bridges (Hedgren (1994)) (see Table 1). The dimensionless height of the end portals (h/L_R) and the step of arch transversal beams (p_{br}/B) are assumed of 0.147 and 0.5, respectively. The cable system consists of 18 hanger elements equally spaced along the girder every 7.5 m. The hangers can be arranged in vertical or net-

Table 3. A description of methodology used to evaluate the nonlinear behavior of tied-arch bridges

1. Definition of the tied arch bridge structure
2. Perform EBA to identify the critical mode shapes of the structure.
2.1. Define the initial configuration of the structure under the action of Dead Loads (DL)
2.2. Resolve the eigenvalue buckling problem
3. Perform NEA
3.1. Define the initial configuration of the structure under the action of DL
3.2. Assign initial out-of-plane displacements, evaluated by means of EBA (point 2)
3.3. Increase live loads (LL) and evaluate the maximum loading capacity of the structure

Table 4. Cross-sections dimension for a tied-arch bridge with L= 150 m

Structural element	Shape	B (mm)	H (mm)	t_f (mm)	t_w (mm)	D (mm)	t_p
Arch Rib	Rectangular	930	930	40	40		
Tie girder	Rectangular	930	2570	40	110		
Arch-cross beams	Pipe					650	10
Hangers	Circular					70	

work configurations. In the last case, the hangers are spit in two specular sub-systems of 9 elements, inclined of an angle α^C with respect to the horizontal. Dead loads, concerning structural and nonstructural loads, are equal to 200 kN/m, whereas live loads are assumed of 160 kN/m, which consists of two lines of the LM-71 train model (European Committee for Standardization (2003)) acting on the whole bridge length. The nonlinear behavior of the structure was investigated by means of a combined analysis method based on Eigenvalue Buckling analysis (EBA) and Nonlinear Elastic Analysis (NEA).

At first, comparisons are proposed between results relatives to bridge configurations with vertical and inward-inclined arch ribs. The analysis was performed considering moment tied configuration and Vierendeel scheme for cable system and wind bracing system, respectively. Fig. 2-a reports the evaluation of the maximum live load multiplier obtained by means of EBA and NEA, whereas Fig. 2-b depicts the first critical mode shapes obtained by means of NEA. Note that, the results of NEA in Fig.2-a are presented in terms of load-displacement curves in the form λ vs δ/L, where λ and δ/L represent the live load multiplier and the normalized out-of-plane displacement of the rib cross-section at x/L=1/4, respectively. The results show that EBA overestimates the maximum capacity of the bridge structures, thereby denoting how nonlinearities of the structure considerably affect the out-of-plane buckling behavior. In particular, the buckling load evaluated by means of EBA is higher than the one obtained by NEA for vertical and inclined arch ribs of 125% and 43%, respectively. Consequently, an accurate evaluation of the buckling capacity of the structure can be achieved exclusively by using NEA analysis.

The results also highlight that arch ribs inclination significantly improves the integrity of the structures against out-of-plane buckling mechanisms since the live load multiplier predicted by NEA increases from 1.34 to 4.33. Such

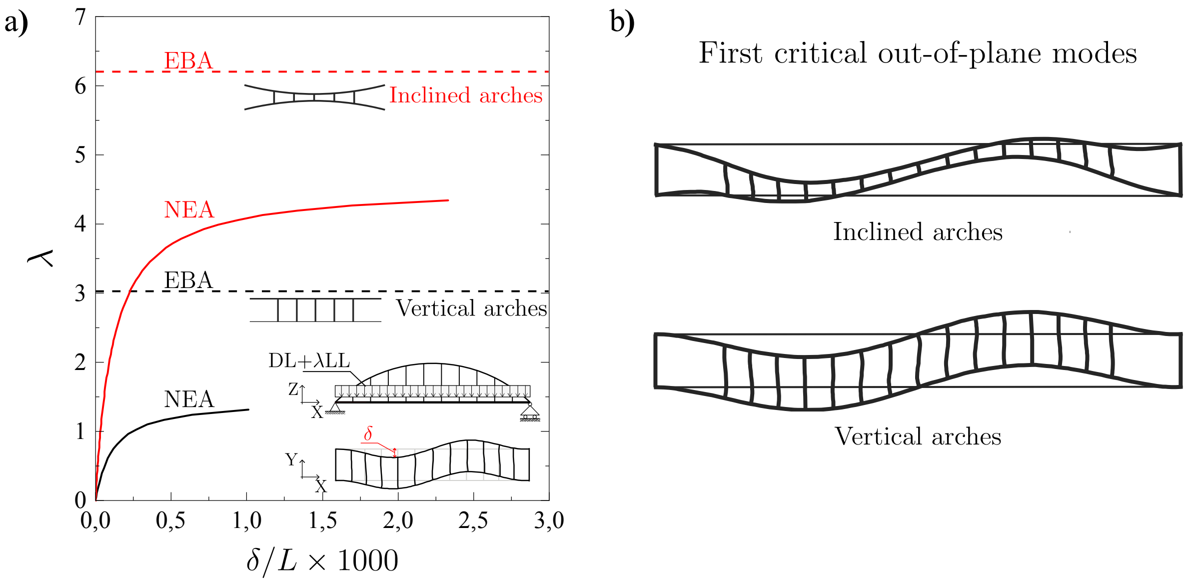

Fig. 2. Comparison between inclined and vertical arch ribs configurations. (a) Maximum live load multiplier (λ) evaluated by means of EBA and NEA; (b) First critical out-of-plane buckling mode shapes predicted by NEA

behavior can be explained by analyzing the buckling modes and the deformed shapes at failure reported in Fig. 2-b. In the case of inclined arches, the center of the structure behaves rigidly, whereas the side zones are affected by relevant lateral displacements as well as larger bending deformations. In this framework, the out-of-plane buckling length of the ribs is considerably reduced and the integrity of the structure improves largely. This mechanism similarly occurs in traditional tied-arch bridge structures with vertical ribs braced by means of X-shaped or K-shaped wind bracing systems, as highlighted in (Lonetti and Pascuzzo (2019); Lonetti et al. (2019)). In particular, in (Lonetti et al. (2019)) the Authors have revealed that the braced portion of the arch ribs behaves as a high stiff truss structure, while the side zones work as portals (*i.e*. the end portals of the structure). In particular, they have found that the minor height of the portals the major integrity of the structure against out-of-plane buckling phenomena. On the other hand, the results relatives to the bridge with vertical ribs reveal that the deformation of the structure is mainly dominated by arch ribs, and no rigid regions are present. In particular, the deformed shape of the structure reproduces similarly the out-of-plane buckling mode shape of a single arch with fixed extremities. Figure 3 shows the variability of the maximum axial force in arch ribs (N_{cr}) in terms of the arch slope α^R. N_{cr} is normalized with respect to the yield axial force of the rib cross-section (N_y), which is defined assuming a yield strength for the steel of 360 MPa. Comparisons between Viereendel and K-shaped wind bracing system schemes are also proposed. The results show that the arch rib inclination significantly improves the integrity of the structure braced by means of Vierendeel bracing system since N_{cr}/N_y largely increases for α^R increments. In particular, the out-of-plane buckling crisis of the structure is completely avoided for α^R >8. On the other hand, the K-shaped bracing system guarantees margin of safety against out-of-plane buckling crisis for any values of slope α^R. In particular, N_{cr}/N_y keeps almost constant with α^R and equal to 2.1. A possible explanation for this might be that the K-shaped bracing system stiffs the ribs so hard to make quite negligible the stiffness provided by arch ribs inclination.

It is worth noting that, the structural integrity of tied-arch bridges with vertical ribs braced by means of a K-shaped bracing system highly depends on the lateral stiffness of the bridge end portals. Fixed joint connections between rib and tie extremities are usually employed to configure end portals with an enhanced lateral stiffness. However, rigid connections may require a considerable amount of economic resources to be realized. Alternatively, hinges joints may be adopted, but the integrity of the structure against out-of-plane buckling phenomena might be considerably reduced. In order to evaluate the structural behavior of tied-arch bridges with fixed and hinge joint connections between rib and tie extremities, further results are developed. In particular, comparisons results are performed between vertical and

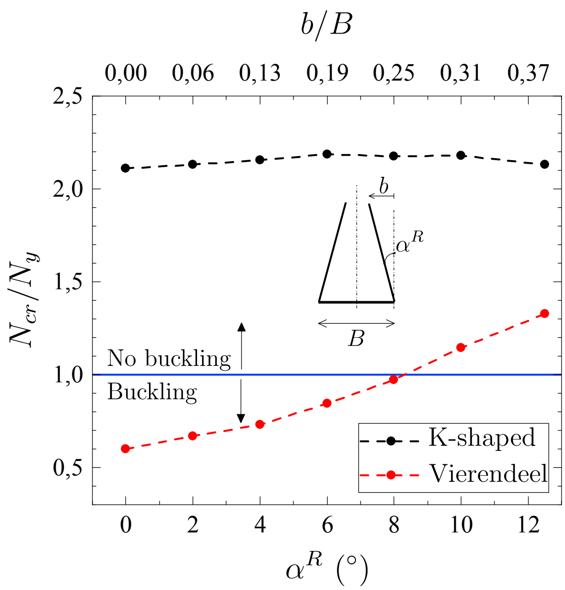

Fig. 3. Variability of the ratio between the critical buckling force N_{cr} and the yield force N_y for several values of the arch ribs inclination (α^R). Comparisons between K-shaped and Vierendeel wind bracing system configurations

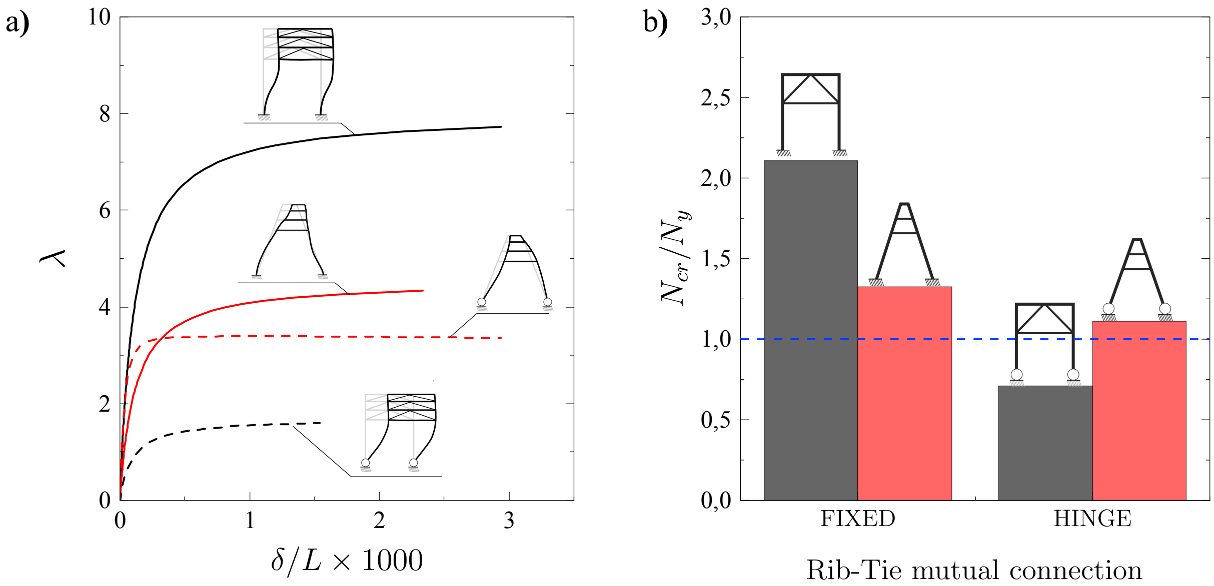

Fig. 4. Effect of joint connection between rib and tie extremities. (a) Load-displacements curves relatives to bridge structure with vertical and inclined arch ribs braced by means of K-shaped and Vierendeel system, respectively. (b) Variability of the arch rib critical axial force

inclined arch ribs configurations braced by means of K-shaped and Vierendeel wind bracing systems, respectively. Figure 4-a depicts the load displacement curves, whereas Fig. 4-b show the corresponding values of critical axial force of ribs normalized with respect to the yield axial force (N_{cr}/N_y). The results show that the performances of K-shaped bracing system suddenly decrease when hinges are adopted since the maximum load multiplier and the corresponding critical axial force reduces about 67%. Contrarily, for the structure with inclined ribs, this decrement is exclusively of 23%. This behavior may be explained by the fact that rib inclination leads to a bridge structure characterized by A-shape transversal geometrical configuration, which provides a notable lateral stiffness mainly due to its geometry. In this framework, fixed or hinge mutual connections between rib and tie extremities less affect the nonlinear behavior of the structure. This can be easily appreciates by means of deformed shape configuration of the structures reported in Fig. 4-a.

The behavior of the structure is now investigated considering the effect arising from both arch rib and hanger inclinations. Figure 5 plots the variability of the live load multiplier of the structure as a function of the hanger slope (α^C), for vertical and inclined arch rib configurations. For the structure with inclined arches, the results show that the live load multiplier varies in a nonlinear manner. In particular, it firstly increases up to a peak value that occurs at α^C=55° and subsequently decreases linearly. This does not occur in the case of vertical arch ribs scheme since the live load multiplier keeps almost constant with the hanger slope. The results indicate that network layouts for the cable system may effectively contribute to increase the performance of tied-arch bridges with inclined ribs.

Finally, a parametric study in terms of bridge length span (L) was performed. The main aim is to assess the effectiveness of this design strategy for bridge spans longer than 150 m, from both structural and economic points of view. In particular, with regard to the economic aspect, the study focuses attention on the overall amount of steel involved in the bracing system (V^{br}), which represents one of the most expensive parts of the entire structure due to high cost of manufacturing processes per unit of volume. For every span length considered, the structures were dimensioned according to the mean values reported in Table 1 and Table 2. Figures 6-a and b show the variability of N_{cr}/N_y and V^{br} as a function of L, respectively. Results obtained for tied-arch bridges with vertical arches braced by means of a K-shaped bracing system are also reported for comparison purpose. Arch ribs inclination can be efficiently employed in the field of medium/large span length because N_{cr}/N_y is almost 1.3 for any value of L. Furthermore, it ensures significant economic benefits since the overall amount of material needed for the bracing system is lower than that

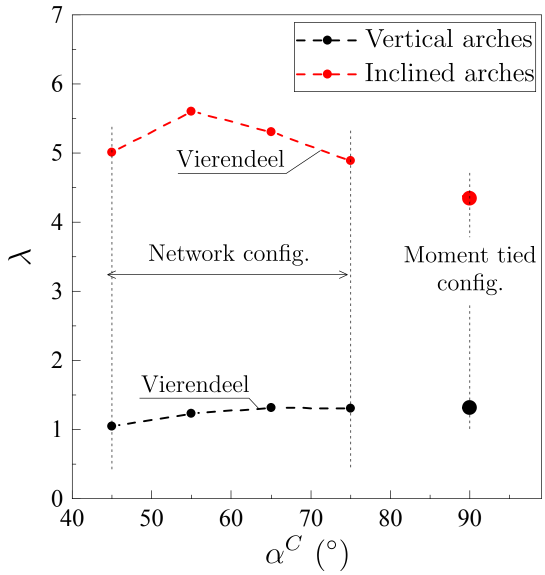

Fig. 5. Variability of the live load multiplier as a function of the hangers slope (α^C)

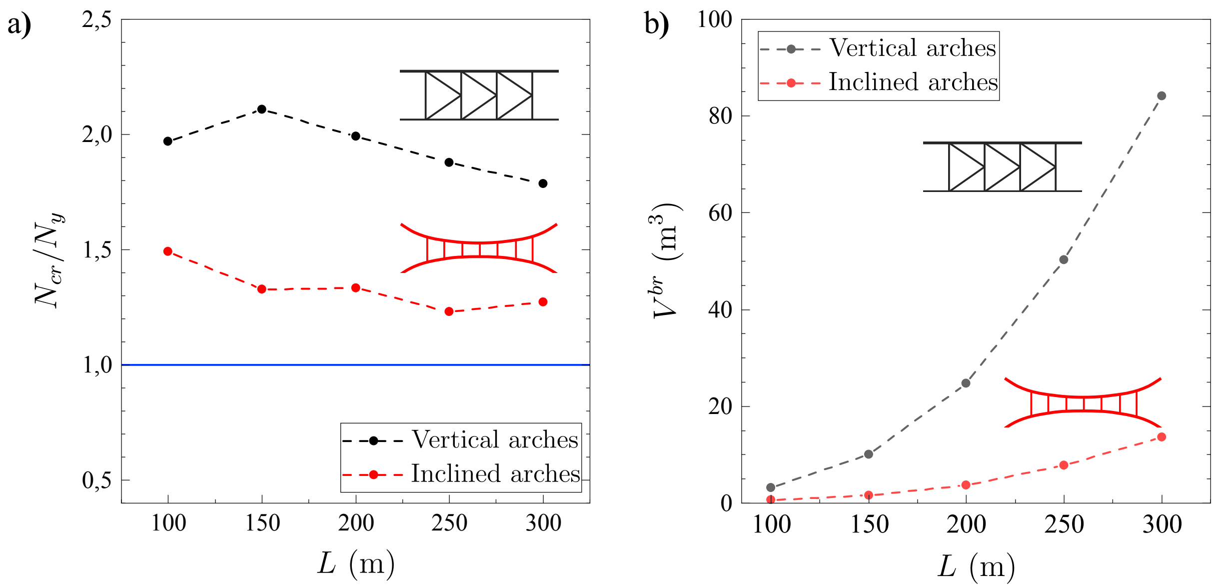

Fig. 6. Comparison between tied arch bridges with inclined and vertical arch ribs for several bridge span lengths (L). (a) Variability of the critical axial force of arch ribs and (b) the volume of the material involved in the wind bracing system (V^{br})

required for the traditional scheme based on vertical arches for every value of L. In particular, the material saving increases exponentially with bridge span length increments.

4. Conclusion

This study examined the effectiveness of arch rib inclination as strategy design to increase the structural integrity of the tied-arch bridges against out-of-plane buckling mechanisms. The analysis was performed by means of a refined FE numerical model, in which an accurate description of any source of nonlinearity involved in structural elements was considered. A method that combines results relative to traditional elastic buckling analysis and incremental nonlinear elastic analysis was adopted to properly quantify the maximum capacity of the bridge structure. An adequate evaluation of the effective capacity of tied-arch bridges can be obtained exclusively by means of nonlinear incremental analyses, since traditional elastic buckling methods may lead to considerable overestimations of the structural capacity. The results denoted that arch rib inclination significantly improves the integrity of the structure against out-of-plane buckling mechanisms. This may be attributed to two main factors. Firstly, the rib inclination generates a high stiff region along the center of the structure, which limits the out-of-plane deformability of the ribs. The effective buckling length of the ribs is then considerably reduced and the integrity of the structure increases. Secondly, the rib inclination configures an A-shape transversal scheme for the structure, which enhances the overall lateral stiffness of the bridge structure mainly by means of its geometry. This mechanism makes tied-arch bridges particularly efficient when hinges are assumed as mutual connections between rib and tie cross-section extremities. Finally, the results have shown that configurations with inclined arch ribs represent an effective solution in the field of long spans, ensuring both structural and economic advantages. From an economic point of view, the amount of material needed for the bracing system is significantly lower than that required for traditional tied arch bridges with vertical arches braced by means of K-shaped systems, thus involving a relevant reduction of construction costs.

References

Backer, H.D., Outtier, A., Bogaert, P.V., 2014. Buckling design of steel tied-arch bridges. Journal of Constructional Steel Research 103, 159 – 167. doi:https://doi.org/10.1016/j.jcsr.2014.09.004.

Bruno, D., Lonetti, P., Pascuzzo, A., 2016. An optimization model for the design of network arch bridges. Computers and Structures 170, 13 – 25. doi:https://doi.org/10.1016/j.compstruc.2016.03.011.

Bruno, D., Lonetti, P., Pascuzzo, A., 2018. A numerical study on network arch bridges subjected to cable loss. International Journal of Bridge Engineering 6, 41–59.

European Committee for Standardization, 2003. EN 1991-2:2003: Eurocode 1: Actions on structures. Part 3: Traffic Loads on Bridges. European Committee for Standardization.

European Committee for Standardization, 2006. EN 1993-2:2006: Eurocode 3. Design of steel structures. Part 2: Steel bridges. European Committee for Standardization.

Greco, F., Lonetti, P., Pascuzzo, A., 2013. Dynamic analysis of cable-stayed bridges affected by accidental failure mechanisms under moving loads. Mathematical Problems in Engineering 2013. doi:10.1155/2013/302706.

Greco, F., Lonetti, P., Pascuzzo, A., 2018. A moving mesh fe methodology for vehicle–bridge interaction modeling. Mechanics of Advanced Materials and Structures 0, 1–13. doi:10.1080/15376494.2018.1506955.

Greco, F., Lonetti, P., Pascuzzo, A., 2019. Structural integrity of tied arch bridges affected by instability phenomena. Procedia Structural Integrity 18, 891 – 902. doi:10.1016/j.prostr.2019.08.240. 25th International Conference on Fracture and Structural Integrity.

Gui, C., Lei, J., Yoda, T., Lin, W., Zhang, Y., 2016. Effects of inclination angle on buckling of continuous composite bridges with inclined parabolic arch ribs. International Journal of Steel Structures 16, 361–372. doi:10.1007/s13296-016-6009-x.

Ştefan Guţiu, Moga, P., Moga, C., Danciu, A., 2016. The new arch bridge in the city of sibiu, romania. Procedia Engineering 156, 132 – 139. doi:https://doi.org/10.1016/j.proeng.2016.08.278. bridges in Danube Basin 2016 – New trends in bridge engineering and efficient solution for large and medium span bridges.

Guo, Y.Z., Liu, A.R., Yu, Q.C., 2012. The effect of inclined arch rib on the dynamic stability of leaning-type arch bridge under earthquake, in: Advanced Building Materials and Structural Engineering, Trans Tech Publications Ltd. pp. 579–581. doi:10.4028/www.scientific.net/AMR.461.579.

Hedgren, A., 1994. Structural Steel Designer's Handbook: Arch Bridges. McGraw-Hill Education.

Ju, S., 2003. Statistical analyses of effective lengths in steel arch bridges. Computers and Structures 81, 1487 – 1497. doi:https://doi.org/10.1016/S0045-7949(03)00061-0.

Lan, K., Hanbin, G., Kazuya, M., Tetsuya, N., 2019. Behavior of a steel bridge with large caisson foundations under earthquake and tsunami actions. Steel and Composite Structures 31, 575–589.

Latif, M., Saka, M., 2019. Optimum design of tied-arch bridges under code requirements using enhanced artificial bee colony algorithm. Advances in Engineering Software 135, 102685. doi:https://doi.org/10.1016/j.advengsoft.2019.102685.

Liu, A., Huang, Y., Yu, Q., Rao, R., 2014. An analytical solution for lateral buckling critical load calculation of leaning-type arch bridge. Mathematical Problems in Engineering 2014, 1–14. doi:10.1155/2014/578473.

Lonetti, P., Maletta, R., 2018. Dynamic impact analysis of masonry buildings subjected to flood actions. Engineering Structures 167, 445 – 458. doi:https://doi.org/10.1016/j.engstruct.2018.03.076.

Lonetti, P., Pascuzzo, A., 2014a. Design analysis of the optimum configuration of self-anchored cable-stayed suspension bridges. Structural Engineering and Mechanics 51, 847–866. doi:10.12989/sem.2014.51.5.847.

Lonetti, P., Pascuzzo, A., 2014b. Optimum design analysis of hybrid cable-stayed suspension bridges. Advances in Engineering Software 73, 53 – 66. doi:https://doi.org/10.1016/j.advengsoft.2014.03.004.

Lonetti, P., Pascuzzo, A., 2014c. Vulnerability and failure analysis of hybrid cable-stayed suspension bridges subjected to damage mechanisms. Engineering Failure Analysis 45, 470 – 495. doi:https://doi.org/10.1016/j.engfailanal.2014.07.002.

Lonetti, P., Pascuzzo, A., 2016. A numerical study on the structural integrity of self-anchored cable-stayed suspension bridges. Frattura ed Integrita Strutturale 10, 359–376. doi:10.3221/IGF-ESIS.38.46.

Lonetti, P., Pascuzzo, A., 2019. A practical method for the elastic buckling design of network arch bridges. International Journal of Steel Structures doi:10.1007/s13296-019-00282-8.

Lonetti, P., Pascuzzo, A., Aiello, S., 2019. Instability design analysis in tied-arch bridges. Mechanics of Advanced Materials and Structures 26, 716–726. doi:10.1080/15376494.2017.1410911.

Lonetti, P., Pascuzzo, A., Davanzo, A., 2016. Dynamic behavior of tied-arch bridges under the action of moving loads. Mathematical Problems in Engineering 2016. doi:10.1155/2016/2749720.

Pellegrino, C., Cupani, G., Modena, C., 2010. The effect of fatigue on the arrangement of hangers in tied arch bridges. Engineering Structures 32, 1140 – 1147. doi:https://doi.org/10.1016/j.engstruct.2009.12.040.

Tan, Y., Yao, Y., 2019. Optimization of hanger arrangement in pedestrian tied arch bridge with sparse hanger system. Advances in Structural Engineering 22, 2594–2604. doi:10.1177/1369433219849842.

Tetougueni, C., Zampieri, P., Pellegrino, C., 2019. Lateral structural behavior of steel network arch bridges, pp. 5834–5841. doi:10.7712/120119.7349.20843. 7th International Conference on Computational Methods in Structural Dynamics and Earthquake Engineering Methods in Structural Dynamics and Earthquake Engineering.

Tetougueni, C., Zampieri, P., Pellegrino, C., 2020. Lateral Stability of Network Arch Bridges. pp. 358–365. doi:10.1007/978-3-030-29227-0_37. proceedings of ARCH 2019.

Tetougueni, C.D., Zampieri, P., 2019. Structural response of cable-stayed bridge subjected to blast load. Procedia Structural Integrity 18, 765 – 774. doi:https://doi.org/10.1016/j.prostr.2019.08.225. 25th International Conference on Fracture and Structural Integrity.